J Mater Sci: Mater Med (2008) 19:3507–3514
DOI 10.1007/s10856-008-3501-7

Bone-like apatite layer formation on the new resin-modified glass-ionomer cement

Jhamak Nourmohammadi · S. K. Sadrnezhaad · A. Behnam Ghader

Received: 2 May 2008 / Accepted: 6 June 2008 / Published online: 15 July 2008

Abstract In this study, the apatite-forming ability of the new resin-modified glass-ionomer cement was evaluated by soaking the cement in the simulated body fluid. The Fourier Transform Infrared (FTIR) spectrometer and X-Ray Diffraction (XRD) patterns of the soaked cement pointed to the creation of poorly crystalline carbonated apatite. It was found that the releasing of calcium ions from the soaked cement will dominate the undesirable effect of polyacrylic acid on apatite formation. Consequently, the ionic activity products (IAPs) of the apatite in the surrounding medium increased which accelerated apatite nucleation induced by the presence of the Si–OH and COOH groups. Accordingly, the apatite nuclei started to form via primary heterogeneous nucleation and continued by secondary nucleation. Therefore, nucleation and growth occurs as in the layer-by-layer mode so that finite numbers of monolayers are produced. Subsequent formation of film occurs by formation of discrete nuclei (layer-plus-island or SK growth).

1 Introduction

Glass polyalkenoates or Glass-Ionomer Cements (GIC) have been used in dentistry for over 30 years due to their ability to adhere to both enamel and dentin and to release fluoride [1, 2]. However, glass-ionomer cement is quite a brittle material and its mechanical properties are limited. In the late 1980s the Resin-Modified Glass-Ionomer Cement (RMGIC) was developed. This kind of glass-ionomer cement has been shown advantageous mechanical properties compared with conventional GICs [3].

Both types of glass-ionomers (GICs and RMGICs) are actually unique organic/inorganic composites that the composition of the inorganic parts in both of the cements is basically the same and composed of basic glass such as calcium fluoro-alumino-silicate powder. The liquid parts of the RMGIC are different and contain not only the polyacid but also a water-compatible monomer which is Hydroxyl-ethylmethacrylate (HEMA) together with polymerization initiators. So, the set RMGIC consists of residual glass particles embedded in a mixed polysalt and polymerized monomer matrix [4, 5].

In spite of other bone cements such as polymethyl-methacrylate (PMMA), glass-ionomer cements set rapidly without any shrinkage and increasing temperature during setting [6, 7]. The trials of implantation of glass-ionomer cements have been conducted; and it has been revealed that GICs couldn't bond chemically to bone such as bioactive materials. On the other hand, even if glass-ionomer cements bond to bone directly, this bonding is not chemical and is attributed to weak mechanical interlocking [8, 9]. It is considered that the essential requirement for an artificial material to bond chemically to bone is to form an apatite layer on its surface [10, 11].

The fundamental understanding of the mechanism of the apatite formation on the surfaces of the $CaO–SiO_2$ based glasses and glass-ceramics in the body provides the way for forming bone-like apatite layer on the surfaces of various kinds of materials including metals, ceramics and organic polymers by the biomimetic process in the Simulated Body Fluid (SBF) [12–14].

It has been reported that Si–OH [15] and –COOH [16] groups play an effective role in heterogeneous nucleation of apatite in the body environment. However, in glass-ionomer

J. Nourmohammadi (✉) · S. K. Sadrnezhaad · A. Behnam Ghader
Biomaterial Department, Material and Energy Research Center, P.O. Box 14155-4777, Tehran, Iran
e-mail: Jhamak_n@yahoo.com

cements, Si–OH and –COOH groups are abundant on the surfaces of the glass particles and in the polyacrylic acid, respectively. So, we expected that GICs could form apatite layer on its surface and formed bioactive cement. A few studies have been applied to evaluate the possibility of obtaining bioactive glass-ionomer cement. Matsuya et al. reported a new glass-ionomer cement based on $CaO–P_2O_5–SiO_2–MgO$ bioactive glass and polyacrylic acid but after immersing this new cement in the simulated body fluid they found no apatite formation on its surface after 4 weeks [17]. Kamikitahara et al. in their studies on the one kind of conventional glass-ionomer cement (Shofa Inc., Japan) concluded that it might be difficult to obtain the bioactive glass-ionomer cement due to release of polyacrylic acid [9].

Thus, we thought that we still need to study on the developing of bioactive glass ionomer cement to expand their applications in the other field of medicine. Therefore, we considered to investigate the formation of apatite layer on the surface of resin-modified glass-ionomer cement because of better mechanical properties and less amount of polyacrylic acid in their composition in compare with conventional glass ionomer cements. So, in the present study formation of an apatite layer on the surface of a new resin-modified glass-ionomer cement to obtain a bioactive cement was investigated.

2 Materials and methods

2.1 Preparation of glass

The glass was prepared from mixtures of finely powdered silica >99.9% pure (Iran, Hamedan), $Al(OH)_3$ (Merck, 1091, Germany), $CaHPO_4 \cdot 2H_2O$ (Merck, 2146, Germany), $CaCO_3$ (Merck, 2064, Germany) and CaF_2 (Merck, 2840, Germany). Table 1 shows the batch composition of the glass.

The pre-fired batch was then placed in a covered alumina crucible and heated in an electric furnace at 1,450°C for two hours. The glass melt was then quickly water-cooled to produce a granular frit. The obtained frit was then ground and sieved to remove particles over 45 μm. The new glass was then analyzed by using X-ray fluorescence spectroscopy (ARL XRF-8410) to determine the concentrations of elements present in the material sample (Table 1).

Table 1 XRF data comparing the chemical composition of the studied glass before and after synthesis

Oxides	Weight percent (wt. %)	
	Pre-melt glass composition	Post-melt glass composition
SiO_2	25.91	24.25
Al_2O_3	29.36	28.23
P_2O_5	13.63	12.28
CaO	16.12	15.99
CaF_2	14.97	12.79

2.2 Cement preparation

The prepared glass powder and a commercial resin-modified glass-ionomer liquid, Fuji II LC (Improved, batch number 609211, GC Corp., Tokyo, Japan), were mixed at room temperature with a powder to liquid ratio of 2.5 using plastic spatula on a Teflon plate for 40 s. The obtained paste was then placed into the Teflon mould of appropriate dimension, covered with polyethylene strips and held within clamps for 30 s. Afterward, the resin cement was cured using a photo-curable lamp (Farazmehr, Esfahan, Iran) with exposure of each end of the specimens for 2 min. Then the final cement was ejected from the mould.

2.3 Soaking in simulated body fluid (SBF)

The SBF was prepared by dissolving the reagent-grade NaCl (Merck, 6400, Germany), $NaHCO_3$ (Merck, 6323, Germany), KCl (Merck, 4935, Germany), $K_2HPO_4 \cdot 3H_2O$ (Merck, 5099, Germany), $MgCl_2 \cdot 6H_2O$ (Merck, 5833, Germany), Na_2SO_4 (Merck, 13462, Germany), $CaCl_2$ (Merck, 2387, Germany) into de-ionized water, and buffered with Tris (Hydroxy-methyl-amino-methane) ($(CH_2OH)_3CNH_2$; Merck, 8387, Germany) and Hydrochloric acid (HCl; Merck, 314, Germany) to pH 7.4 at 37°C [18]. The concentration of different ionic species in SBF closely resembles with that of human blood plasma, as listed in Table 2.

Each cement was immersed in 30 ml of SBF in the polyethylene bottles and kept at 37°C in an incubator for 1, 7, 14 and 28 days. The SBF was renewed each 24 h. At the

Table 2 Ion concentration of SBF in comparison with human blood plasma

Ion species	Ion concentration (mM)	
	SBF solution	Human blood plasma
Na^+	142.0	142.0
K^+	5.0	5.0
Mg^{2+}	1.5	1.5
Ca^{2+}	2.5	2.5
Cl^-	148.8	103.0
HCO_3^-	4.2	27.0
HPO_4^{2-}	1.0	1.0
SO_4^{2-}	0.5	0.5

end of the immersion periods, the samples were removed from the SBF, gently washed with de-ionized water and dried at room temperature.

2.4 Analysis of solid and solution

The surface morphologies of specimens before and after soaking in SBF were examined by Scanning electron microscopy (SEM; CAMBRIGE S360, England) using carbon coating. Composition of the specimens was measured by an Energy dispersive spectroscopy (EDS) in the SEM. In addition, the samples were studied by the contact Atomic force microscopy (AFM) analysis using a Park CP instrument (Park Scientific Instruments). The measurements were performed in constant force mode in air with silicon nitride tips from Park. In order to check the absence of precipitation in solution, a laser beam pointer of 1 mW was directed in the SBF. The scattering of the red laser beam indicated the precipitation of calcium phosphate.

XRD spectra were obtained using Philips PW 3710 X-ray diffractometer (CuKα radiation, 40 kV and 30 mA). Data were collected in the range of $2\theta = 20$–40 using 0.01 step and 0/00058 /s scanning speed.

FTIR spectra of the cement powder before and after 4 weeks immersion in the SBF were recorded with a Fourier transform infrared (FTIR) spectrometer (Bruker Vector 33, Germany) in the range of 4,000–400 cm^{-1} to evaluate the calcium phosphate formation. Pellets were prepared for FTIR measurement by mixing dried cement powder with spectroscopic grade KBr and then compressing the mixtures to form pellets for measurements. All measurements were at a 4 cm^{-1} resolution. Changes in the pH of the SBF due to the immersion of the resin-modified glass-ionomer cement were measured using a pH meter (ΩMetrohm 827 pH lab, Swiss). The amount of Ca^{2+} and P^{5+} ions of the SBF is determined by Inductive couple plasma (ICP;model ARL-3410).

3 Results

The XRD patterns of the cement in the range of $2\theta = 20$–40, shown in Fig. 1, consists of numerous sharp peaks indicative of crystalline hydroxyapatite with major peak at d = 2.81, 2.72 and 2.78 with hexagonal symmetry and a-axis = 9.4166 and c-axis = 6.8745 (JCPDS standard 84-1998). By increasing the immersion time up to 28 days, the XRD data revealed a number of significant aspects.

First, there was no obvious indication of peaks other than hydroxyapatite, which suggests that hydroxyapatite layer formed on the surface of cements.

Second, the intensity of the peaks declined as time passed, which is indicative of thickening of the formed

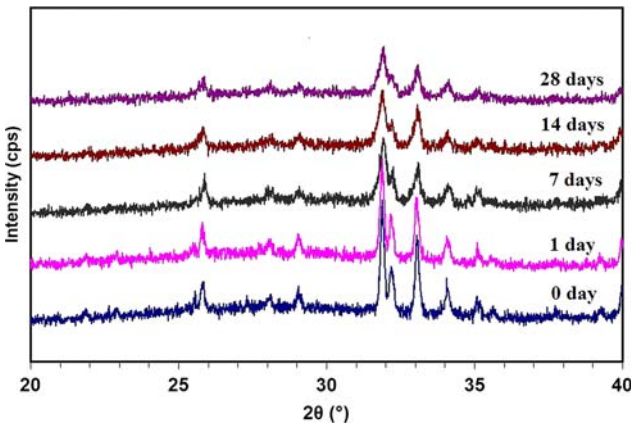

Fig. 1 XRD patterns of the surfaces of resin-modified glass-ionomer cement soaked in SBF for various periods

layer on the surface of the cement. Moreover, broadening of the peaks, mainly the (002), (112), (211) and (300) reflection over the period of time suggested that the formed apatite layer on the surface of the cements is poorly crystalline. This supports the recent deduction by Yu et al. [19], which indicate that the apatite layer formed in SBF on the hydroxyapatite/polyetheretherketone biocomposite was of lower crystallinity.

However, the crystallinity degree (X_c), corresponding to the fraction of crystalline phase present in the examined volume was evaluated by the relation [20]:

$$X_c \approx 1 - (V_{112/300}/I_{300})$$

where I_{300} is the intensity of (300) refection and $V_{112/300}$ is the intensity of the hollow between (112) and (300) reflections, which completely disappears in non-crystalline samples. The evaluated degrees of crystallinity for these samples are given in the Table 3.

The calcium phosphate formation was monitored by measuring the calcium and phosphorus concentration as a function of time in SBF. It can be seen from Fig. 2 that their amounts were consecutively increased and decreased until 28 days.

Figure 3 reveals the infrared reflectance spectra of the resin-modified glass-ionomer cement before and after 28 days exposure in SBF in the range of 4,000–400 cm^{-1} at

Table 3 The effect of soaking time on the crystallinity of hydroxyapatite

Time (days)	Crystallinity X_c (%)
0	0.71
1	0.67
7	0.58
14	0.44
28	0.39

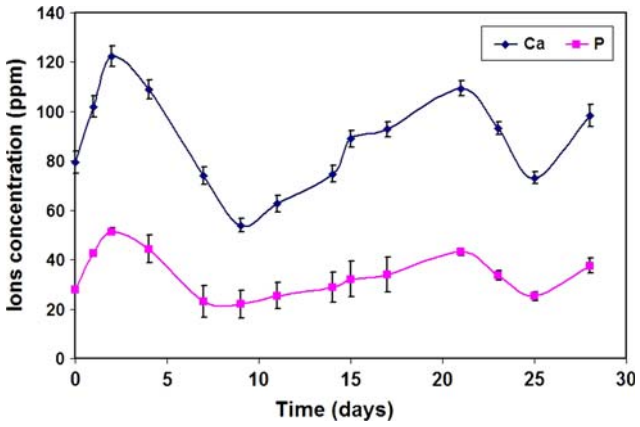

Fig. 2 Changes in calcium and phosphorus concentrations of the SBF with soaking time of resin-modified glass-ionomer cement

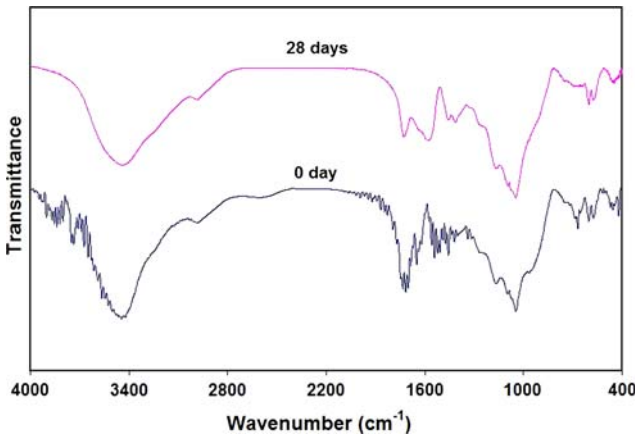

Fig. 3 Change in IR spectra of the experimental cement after 28 days soaking in SBF

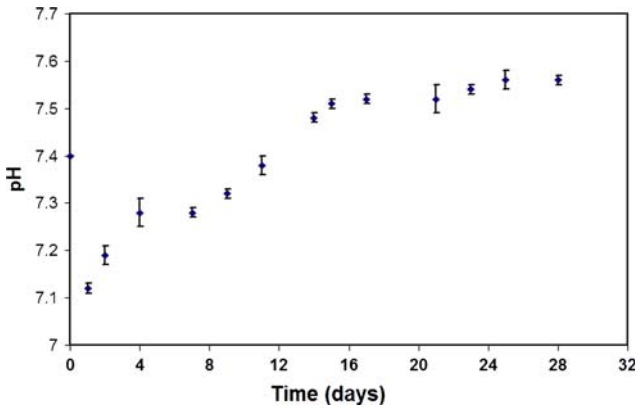

Fig. 4 Change in pH of SBF solution after soaking the resin-modifiied glass-ionomer cements for various time periods

room temperature. The base cement spectra show sharp and well-resolved peaks at 1,100–950 and 650–550 cm^{-1}. The peaks at 1,044, 1,091 and 956 cm^{-1} are assign to υ_3 and υ_1 stretching vibration of PO_4^{3-}, respectively. In addition, the two well-separated peaks at 572 and 600 cm^{-1} both assign to υ_4 mode of PO_4^{3-}. The vibration modes of O-H group at about 3,571 and 639 cm^{-1} also observed in FTIR spectra [21–24]. These peaks showed the presence of hydroxyapatite phase in the cement prior to soaking in SBF. This result is in accordance with the result obtained by XRD patterns. Moreover, the band in the region 1,650–1,550 and 1,440–1,335 cm^{-1} due to the asymmetric and symmetric stretching vibration of COO^- of carboxylic acid salts, were observed [25]. The appearance of those bands revealed that the acid–base reaction also occurred between the glass and polyacids during the setting process. The C=O stretching vibration of ester group of poly HEMA and COOH group in polyacid absorb in the region 1,725–1,700 cm^{-1} [25–27]. The change of the cement composition after 28 days immersion in SBF was also stated by the change of its infrared reflectance pattern. Initially, the amount of the C–O and C=O stretching vibration peaks of polyacids sharply decreased, which suggests that a layer coats the surface of the cement. Subsequently, the bands at 1,453 and 1,413 cm^{-1} come from υ_3 modes of carbonate [21, 28] and are characteristic of carbonate-hydroxyapatite. It can be said that the all carbonate peaks found in the FTIR spectrum of apatite are attributed from precipitated apatite.

As shown in Fig. 4, the pH of SBF decreased swiftly from 7.40 to 7.12 after 1 day of soaking. Later, a steadily increase followed by constant stage (pH 7.56) has been registered.

Figure 5 depicts the topographic profile of the cement surface before and after 1 day immersion in the SBF media. The AFM images of unreacted cement (Fig. 5a) shows glass particles which are surrounded by porous polymer matrix. Soaking in the SBF medium resulted in significant change of surface morphology characterized by peak-to-valley structures. Furthermore, some scattered globules exhibited on its surface suggesting the heterogeneous nucleation of calcium phosphate (light colors in Fig. 5b).

The early events in the nucleation and growth and also change in the morphology of calcium phosphate films on the surface of glass-ionomer cement from immersion time of 1–28 days in SBF solution were investigated by using SEM. Glass particles embedded in the polymeric matrix were visible in the base cement before soaking in the SBF (Fig. 6a). After 1 day of immersion in SBF (pH 7.12), some calcium phosphate deposits were visible on the cement. The calcium phosphate globules scattered on the whole surface of cement. The diameter of these calcium phosphate deposits varied from 80 to 100 nm (Fig. 6b). It seemed to be that larger globules were aggregated and form some small entities.

After 7 days of immersion in SBF (pH 7.28) the whole part of the cement was covered with calcium phosphate film. The film was composed of large calcium phosphate

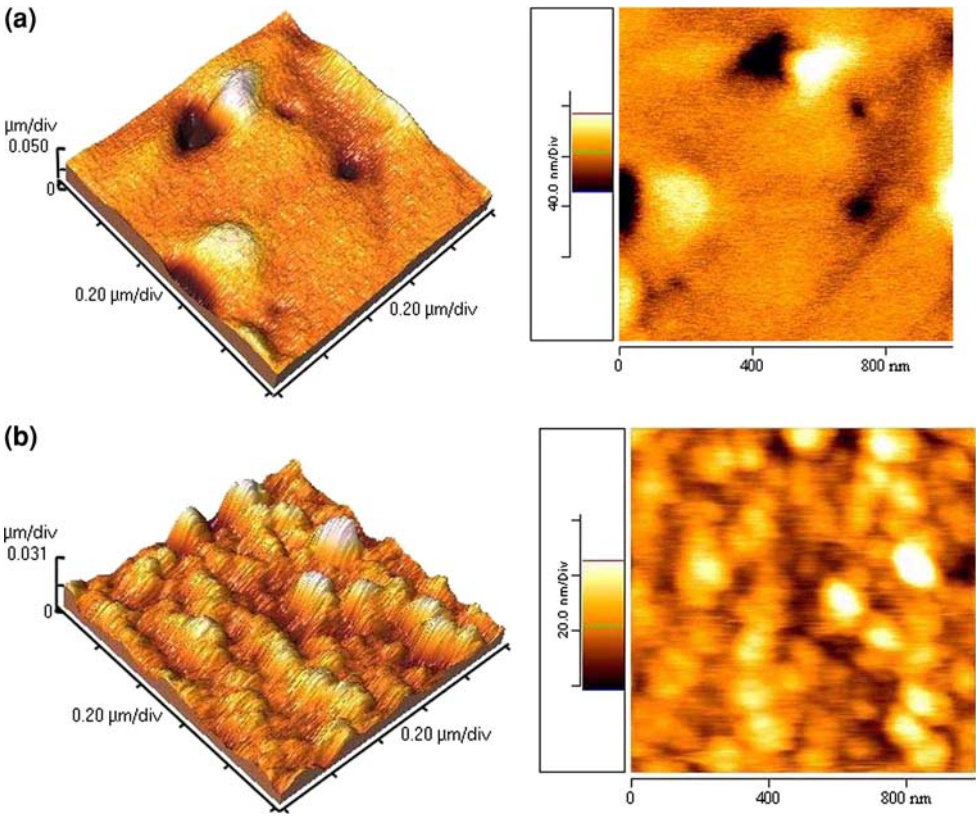

Fig. 5 The feature of the original surfaces of the cement: (**a**) before (**b**) after 1 day soaking

globules linked to each other (Fig. 6c). Again the spherical nucleate form on the surface of the covered film. At this stage, a precipitation was detected in the solution using a laser beam pointer. In fact, the reduction in the amount of calcium ions after 7 days of soaking (Fig. 2) show precipitate was consisted of some small nuclei taken apart from the formed layer.

As indicated in Fig. 6d, after 14 days of immersion (pH 7.47) the rod shape units appeared on the surface of the cement that in some area joined to each other similar to the root of tree. A lower magnification of this stage shows the formation of some islands on the surface of the experimental cement (Fig. 6e). For longer immersion time up to 28 days (Fig. 6f, pH 7.56), the remaining channels and voids were filled by secondary nucleation, island growth and coalescence. EDAX spectra in Fig. 6a, f confirms enlargement of calcium and phosphorus intensities in comparison with base cement, after 28 days immersion in SBF. However, the change of the phosphorus concentration is more obvious than the calcium concentration. Furthermore, the amounts of aluminum and silicon decrease. As proved by EDAX, a thin layer of calcium phosphate film formed on the surface of the resin-modified glass-ionomer cement immersed for 28 days in SBF.

The XRD pattern of the resulted precipitate after 7 days of soaking, exhibited two wide bumps located at $2\theta = 26$ and 33 . These bumps are characteristics of the broadening apatite diffraction lines indicating a poorly crystallized structure (Fig. 7a). It should be mentioned that the FTIR Spectrum of the precipitate in SBF solution also shows the formation of carbonate apatite phase (Fig. 7b).

The cross-section view of sample after 28 days immersion in SBF, showing interconnected micropores (Fig. 8), Therefore, the calcium phosphate film form not only on the surface of the cement but also inside the cement due to the penetration of SBF inside the pores.

4 Discussion

As revealed by XRD pattern (Fig. 1), crystalline hydroxyapatite (HA) peaks appeared on the experimental cement. This finding is caused by the presence of calcium and phosphate ions in the cement powder. When the polymeric acid mixed with acid-soluble glass, such materials undergo polymerization via a light activated process as well as acid/base reaction during the setting procedure. Therefore, the calcium ions leached out from the glass due to the acid hydrolysis of glass network (Eq. 1) [29–31].

$$\equiv \mathrm{Si} - \mathrm{O} - \mathrm{Ca} - \mathrm{Si} \equiv + 2\mathrm{H}^{+} \rightarrow \mathrm{Ca}^{2+} + 2(\equiv \mathrm{Si} - \mathrm{OH}) \quad (1)$$

Subsequently, some of these calcium ions bind with the phosphate groups in the polysalt matrix of the cement and consequently, formed cement based on calcium phosphate.

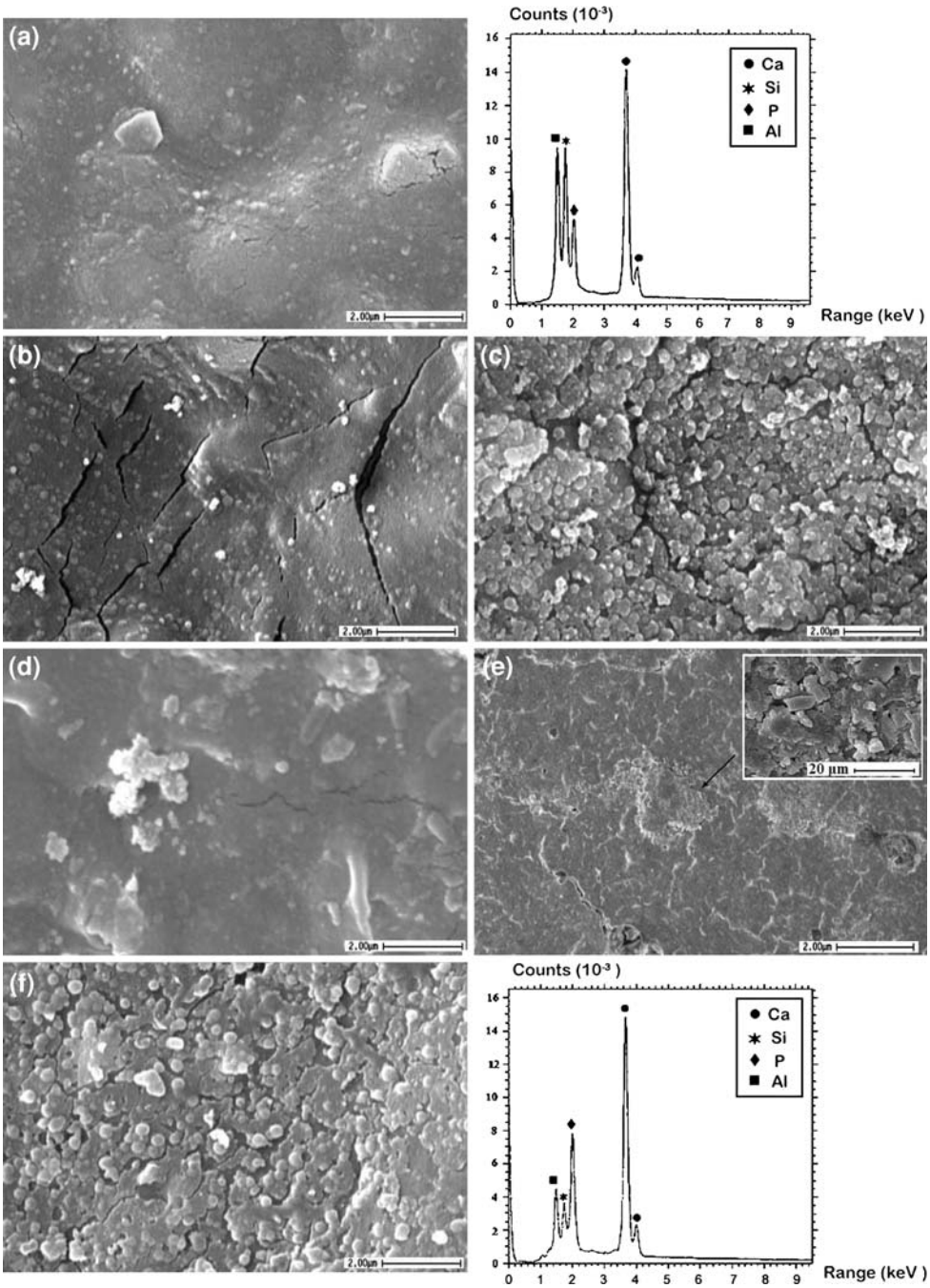

Fig. 6 SEM micrographs and corresponding EDAX spectra of resin-modified glass-ionomer cement versus soaking time in SBF (**a**) 0 day (**b**) 1 day, (**c**) 7 days, (**d**, **e**) 14 days (**f**) 28 days immersion (Magnification = ×10,000 (**a**–**d**, **f**) and ×100 (**e**))

When the set cements were kept in SBF for 28 days the poorly crystalline apatite phase were formed on the surface of the cement. The formation of poorly crystalline apatite is due to the presence of Si–OH and COOH groups in the RMGIC cement. It has been reported that these functional groups are negatively charged in the body environment and act as an inductive factor for apatite nucleation [32, 33]. With due attention to the previous reports about the difficulty of producing bioactive glass-ionomer cement [9], the finding of the present study indicated that the apatite-forming ability of the Si–OH and COOH groups varied with their structures. Indeed, the increase in the calcium ion concentration due to the soaking of the cement further increased the degree of supersaturation (IP/K_0) of SBF with respect to the apatite. It is believed that the crystalline apatite starts to precipitate on the surfaces of the specimens when (IP/K_0) reaches a certain level [34]. Therefore, release of calcium ions from the cement will dominate the inhibitory effect of polyacrylic acid on apatite formation. With time calcium ions from SBF bind with these negatively charged groups and form complexes. Consequently, the complexes incorporate phosphate ions

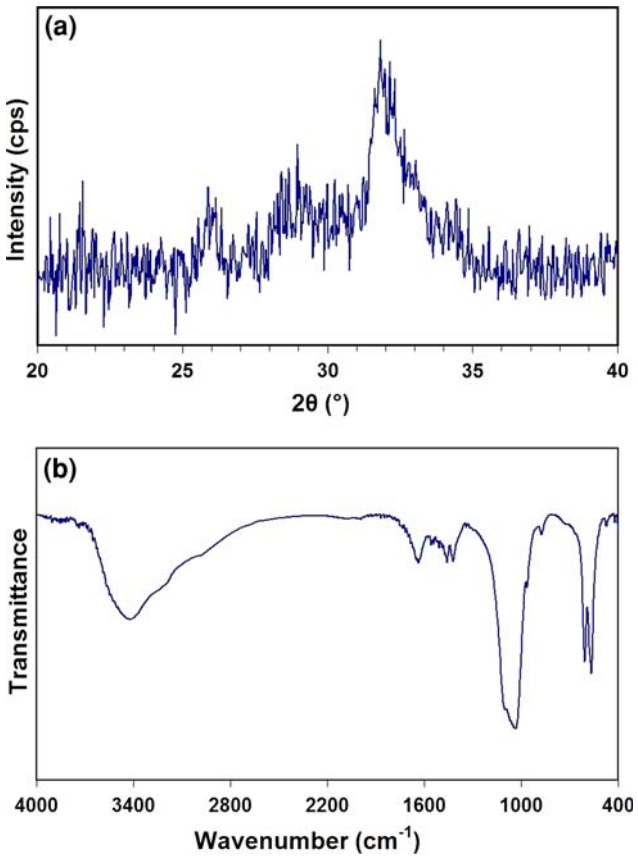

Fig. 7 (**a**) XRD pattern (**b**) FTIR spectrum of the collected precipitate from SBF after 7 days of immersion

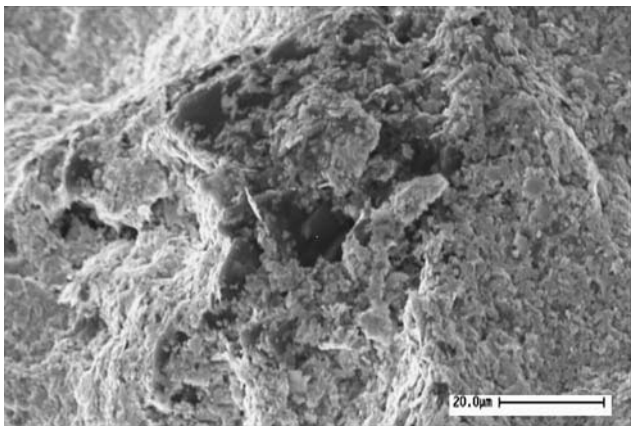

Fig. 8 SEM image showing the presence of interconnected micropores. (Magnification = ×1,000)

to form apatite nuclei. The apatite nuclei grew spontaneously by consuming the calcium and phosphate ions from SBF (Fig. 2). The further increases in calcium and phosphorus concentration after apatite formation are due to the porous structure of the cement. So, the SBF penetrated into the cement and caused the calcium and phosphorus amounts increased again.

The IR spectra of the samples pointed to the formation of B-type carbonate apatite on the experimental cements. This means that carbonate ions (CO_3) occupied the trivalent anionic (PO_4^{3-}) sites of apatite structure. It is generally held that in most low temperature apatites, the CO_3 ions typically substitute for phosphate (PO_4^{3-}) groups [35]. In addition, the XRD pattern and IR spectrum of the resulted precipitate is similar to X-ray diffraction pattern and IR absorption spectrum of human bone mineral. However, bone apatite crystals are carbonate apatite as well as intimately associated with an organic matrix [35, 36].

The pH plot in Fig. 4 shows that acidic ions such as polyacrylic acid (PAA) and phosphates were more released from the cement during the first day of immersion. Moreover, decreasing the amount of pH at the first day of soaking reveals the precipitation of apatite from the SBF. It is clear that during the apatite formation, the hydroxyl groups were consumed from the SBF [36]. So, in accordance to the LeChatelier rule, system goes to the increasing of the amounts of H^+ ions which caused the pH to decline. With time the apatite nuclei grew by consuming the calcium, phosphates and carbonates ions from the SBF. In spite of the leaching of calcium ions from the cement, it is speculated that the most effective factor on the pH rising was absorption of phosphates and carbonates from the SBF. This result is in accordance with the results obtained by FTIR (Fig. 3).

Since, it was so hard to detect these nanometric entities by SEM, the first 24 h events happening on the resin-modified glass-ionomer cement surface have been studied by two complementary microscopes, AFM and SEM. It has been found that nanometric calcium phosphate globules deposits on the surface of the glass-ionomer cement after 1 day immersion in SBF solution (pH 7.12). This implies that chemical affinity of silanol and carboxyl group for forming apatite nuclei resulted in primary heterogeneous nucleation of calcium phosphate. The AFM observations corroborated the finding obtained by SEM. With an increasing immersion time, these units aggregated into large globules via secondary nucleation and consequently expanded on the whole surface of the experimental cement after 7 days of immersion (Fig. 6c). It has to be mentioned that, the nucleation of calcium phosphate should be easier on a surface of the same nature compared to the nucleation on a chemically different surface [37]. On the other hand, some calcium phosphate nuclei have directly formed on the surface of the cement while other clustered on the surface of the primary nuclei to form large globules. With time these secondary globules bond to each other's creating a layer that extended on the RMGIC cement.

The change on the morphology of the resulted phase during the immersion time as revealed by SEM images

(Fig. 6d) is due to the incorporation of carbonate ions into the apatite structure. This is also consistent with previous reports that the addition of carbonate into the apatite structure can influence the structure as well as morphology of the apatite [35, 36]. As revealed by SEM images (Fig. 6) nucleation and growth occurs as in the layer-by-layer mode so that finite numbers of monolayers are produced. Subsequent formation of film occurs by formation of discrete nuclei. The lattice mismatch between the substrate and the created layer cannot be accommodated when the layer thickness increases so that the three-dimensional growth follows the layer-by-layer growth. Alternatively, symmetry or orientation of the over layers with respect to the substrate might be responsible for the production of this growth mode. This kind of growth is known as Stranski-Krastanov growth (layer-plus-island) [38].

5 Conclusion

The present study has shown that poorly crystalline B-type carbonate apatite formed on the whole part of the resin-modified glass-ionomer cement soaked in simulated body fluid (SBF) solution. However, the high chemical affinity of silanol and carboxyl group for forming apatite nuclei accompanied with calcium release from the cement resulted in primary heterogeneous nucleation of calcium phosphate. Subsequently, with time other nuclei clustered on the surface of the primary nuclei via secondary nucleation. These secondary globules bond to each other create a film that is extended on the RMGIC cement. Moreover, this study concludes that the growth of the studied film follows a two step process: initially, complete films of adsorbates to several monolayers thick, grow in a layer-by-layer fashion on the experimental cement. Beyond a critical layer thickness, growth continues through the nucleation and coalescence of adsorbate 'islands'.

References

1. J.W. Nicholson, Biomaterials **19**, 485 (1998). doi:10.1016/S0142-9612(97)00128-2
2. G.J. Mount, Biomaterials **19**, 573 (1998). doi:10.1016/S0142-9612(97)00139-7
3. W. Kanchanavasita, H.M. Anstice, G.J. Pearson, Biomaterials **19**, 1703 (1998). doi:10.1016/S0142-9612(98)00079-9
4. A.D. Wilson, Int. J. Prosthodont. **3**, 425 (1990)
5. G. Palmer, H.M. Anstice, G.J. Pearson, J. Dent. **27**, 303 (1999). doi:10.1016/S0300-5712(98)00058-X
6. P.V. Hatton, K. Hurrell-Gillingham, I.M. Brook, J. Dent. **34**, 598 (2006). doi:10.1016/j.jdent.2004.10.027
7. A.U.J. Yap, Y.S. Pek, R.A. Kumar, P. Cheang, K.A. Khor, Biomaterials **23**, 955 (2002). doi:10.1016/S0142-9612(01)00208-3
8. I.M. Brook, P.V. Hatton, Biomaterials **19**, 565 (1998). doi:10.1016/S0142-9612(98)00138-0
9. M. Kamitakahara, M. Kawashita, T. Kokubo, T. Nakamura, Biomaterials **22**, 3191 (2001). doi:10.1016/S0142-9612(01)00071-0
10. L.L. Hench, J. Am. Ceram. Soc. **74**, 1487 (1991). doi:10.1111/j.1151-2916.1991.tb07132.x
11. T. Kokubo, Biomaterials **12**, 155 (1991). doi:10.1016/0142-9612(91)90194-F
12. C. Ohtsuki, T. Kokubo, T. Yamamura, J. Non-Cryst. Solids **143**, 84 (1992). doi:10.1016/S0022-3093(05)80556-3
13. O.H. Andersson, K.H. Karlsson, J. Non-Cryst. Solids **129**, 145 (1991). doi:10.1016/0022-3093(91)90090-S
14. X. Liu, C. Ding, P.K. Chu, Biomaterials **25**, 1755 (2004). doi:10.1016/j.biomaterials.2003.08.024
15. P. Li, C. Ohtsuki, T. Kokubo, K. Nakanishi, N. Soga, T. Nakamura, T. Yamamuro, J. Am. Ceram. Soc. **75**, 2094 (1992). doi:10.1111/j.1151-2916.1992.tb04470.x
16. M. Tanahashi, T. Matsuda, J. Biomed. Mater. Res. **34**(3), 305 (1997). doi:10.1002/(SICI)1097-4636(19970305)34:3<305::AID-JBM5>3.0.CO;2-O
17. S. Matsuya, Y. Matsuya, M. Ohta, Dent. Mater. J. **18**(2), 155 (1999)
18. T. Kokubo, H. Kushitani, S. Sakka, T. Kitsugi, T. Yamamuro, J. Biomed. Mater. Res. **24**, 721 (1990). doi:10.1002/jbm.820240607
19. S. Yu, K.P. Hariram, R. Kumar, P. Cheang, K.K. Aik, Biomaterials **26**, 2343 (2005). doi:10.1016/j.biomaterials.2004.07.028
20. Y.X. Pang, X. Bao, J. Eur. Ceram. Soc. **23**, 1697 (2003). doi:10.1016/S0955-2219(02)00413-2
21. G. Xu, I.A. Aksay, J.T. Groves, J. Am. Chem. Soc. **123**(10), 2196 (2001). doi:10.1021/ja002537i
22. S.J. Gadaleta, E.P. Paschalis, F. Betts, R. Mendelsohn, A.L. Boskey, Calcif. Tissue Int. **58**(1), 9 (1996). doi:10.1007/BF02509540
23. A.C. Tas, Biomaterials **21**, 1429 (2000). doi:10.1016/S0142-9612(00)00019-3
24. Y. Li, T. Wiliana, K.C. Tam, Mater. Res. Bull. **42**, 820 (2007). doi:10.1016/j.materresbull.2006.08.027
25. G. Socrates, *Infrared and Raman Characteristic Group Frequencies: Tables and Charts* (Wiley, Chichester, 2001)
26. A.M. Young, Biomaterials **23**, 3289 (2002). doi:10.1016/S0142-9612(02)00092-3
27. A.M. Young, S.A. Rafeeka, J.A. Howlett, Biomaterials **25**, 823 (2004). doi:10.1016/S0142-9612(03)00599-4
28. D. Tadic, F. Peters, M. Epple, Biomaterials **23**, 2553 (2002). doi:10.1016/S0142-9612(01)00390-8
29. J. Nourmohammadi, R. Salarian, M. Solati-Hashjin, F. Moztarzadeh, Ceram. Int. **33**, 557 (2007). doi:10.1016/j.ceramint.2005.11.017
30. S. Matsuya, T. Maeda, M. Ohta, J. Dent. Res. **75**(12), 1920 (1996)
31. F. Branda, F. Arcobello-Varlese, A. Costantini, G. Luciani, Biomaterials **23**, 4029 (2002). doi:10.1016/S0142-9612(01)00173-9
32. T. Kawai, C. Ohtsuki, M. Kamitakahara, T. Miyazaki, M. Tanihara, Y. Sakaguchi et al., Biomaterials **25**, 4529 (2004). doi:10.1016/j.biomaterials.2003.11.039
33. O.H. Andersson, K.H. Karlsson, J. Non-Cryst. Solids **129**, 145 (1991). doi:10.1016/0022-3093(91)90090-S
34. H. Kim, F. Miyaji, T. Kokubo, C. Ohtsuki, T. Nakamura, J. Am. Ceram. Soc. **78**(9), 2405 (1995). doi:10.1111/j.1151-2916.1995.tb08677.x
35. S. Sarig, Bone **35**, 108 (2004). doi:10.1016/j.bone.2004.02.020
36. L.L. Hench, J. Wilson, *An Introduction to Bioceramics* (World Scientific, London, 1993), p. 143
37. F. Barrere, M.M.E. Snel, C.A. Blitterswijk, K. De Groot, P. Layrolle, Biomaterials **25**, 2901 (2004). doi:10.1016/j.biomaterials.2003.09.063
38. K.L. Chopra, *Thin Film Phenomena* (McGraw-Hill, New York, 1969)